

Anomalous Mixing Behavior of Polyisobutylene with Other Polyolefins

R. Krishnamoorti[†] and W. W. Graessley*

Department of Chemical Engineering, Princeton University, Princeton, New Jersey 08544

L. J. Fetters, R. T. Garner, and D. J. Lohse

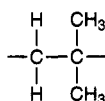
Corporate Research Laboratories, Exxon Research and Engineering Company, Annandale, New Jersey 08801

Received August 4, 1994; Revised Manuscript Received November 21, 1994[®]

ABSTRACT: Mutual solubilities and liquid-state interactions of polyisobutylene (PIB) with other polyolefins were investigated by a variety of techniques. Near room temperature PIB was found to be miscible with a limited range of polyolefin structures. The interactions for several blends in this range were determined by small-angle neutron scattering. The Flory–Huggins parameter χ was found to be large and negative at room temperature in all cases, contrary to expectations and to previous experience with blends of other saturated hydrocarbon polymers. However, χ diminished rapidly in magnitude with increasing temperature, eventually becoming positive and culminating finally in phase separation. Molecular weight independence of χ , volume change on mixing, glass transition temperature *vs* blend composition, and a phase diagram were established for one PIB/polyolefin system. The insensitivity of phase separation temperature to both blend composition and component molecular weight was shown to be a natural qualitative consequence of the unusually strong temperature dependence of χ . The volume changes and T_g behavior are also unusual and remain to be explained, along with the fundamental source of attractive interactions (negative χ) in blends of saturated hydrocarbon polymers.

Introduction

In previous work^{1–8} we have investigated the thermodynamic interactions that govern phase behavior in numerous blends of model polyolefins. The components, obtained by saturating the double bonds of nearly monodisperse polydienes, include a series of statistical ethylene–butene copolymers, an alternating ethylene–butene copolymer, head-to-head as well as head-to-tail polypropylene, and a series of saturated polyisoprenes with varying amounts of 1,4 incorporation. The interactions in their blends, expressed in terms of the Flory–Huggins parameter χ , vary widely in strength and temperature dependence. Classical UCST behavior was found for the majority of component pairs, but the trend with temperature for others suggested LCST or more complex behavior. With only minor exceptions, however, χ was positive over the accessible range of temperatures, indicating a net repulsion between components. Here we report some results obtained for blends of these same model polyolefins with polyisobutylene (PIB), also a saturated hydrocarbon polymer and having the structural unit



In contrast with our previous studies, and contrary to expectations based on the nonspecific (dispersive) nature of saturated hydrocarbon interactions, large *negative* values of χ are found in several of these blends.

Relatively little work has been published on blends of PIB with other polyolefins. Flory et al.⁹ studied the thermodynamics of mixing for solutions of PIB in a

range of linear alkanes, C₅ to C₁₆. They found negative enthalpy and volume changes with mixing that diminished with increasing temperature and alkane size, and they predicted LCST behavior at elevated temperatures. The prevalence of LCST behavior for polymer–solvent systems in general has been related to differences in thermal expansion coefficient through free volume arguments.¹⁰ Flory et al.¹¹ concluded from equation-of-state considerations, based on pure component PVT data, that PIB and polyethylene would be immiscible in the melt state. At least partial miscibility has been suggested for melts of PIB and isotactic polypropylene.¹²

We have used cloud point measurements and visual inspection to survey the miscibility of PIB with a wide range of polyolefins, including both model and commercial materials. Values of $\chi(T)$ were determined for several of these blends by small-angle neutron scattering (SANS). In one case the glass transition temperature and volume change with mixing were measured as functions of blend composition, and an approximate phase diagram was established by a calorimetry–quenching procedure. Equation-of-state contributions to the interactions are briefly considered.

Experimental Section

Structural information and M_w for the polymers used in this work are given in Table 1. Three model PIB samples (PIBA, PIBB, and PIBC) were obtained from American Polymer Standards Corp. All were monomodal and had similar polydispersities ($M_w/M_n \approx 1.2$). Two commercial samples (PIBD and PIBE) were also used, one from BASF (Oppanol B15SF) with $M_w/M_n = 2.35$ and the other from Exxon (Vistanex L100) with $M_w/M_n = 2.0$.

The model polyolefins used as second components in blends with PIB have been described in earlier papers.^{1–8} The first letter of their sample codes is H or D, indicating fully hydrogenous or partially deuterated, and the rest describes the chemical microstructure. The letters A, B, etc. are appended to distinguish different samples with the same microstructure. Thus, H52 is a hydrogenated polybutadiene (a statistical copolymer of ethylene and butene) that contains

[†] Present address: Department of Chemical Engineering, California Institute of Technology, Pasadena, CA 91125.

[®] Abstract published in *Advance ACS Abstracts*, January 15, 1995.

Table 1. Characterization of Samples

sample	description	$M_w \times 10^{-3}$
PIBA	sample from American Polymer Standards	38.6
PIBB	sample from American Polymer Standards	81.6
PIBC	sample from American Polymer Standards	160
PIBD	commercial PIB from BASF	122
PIBE	commercial PIB from Exxon	1000
H38 (D38)	model ethylene-butene (EB) copolymer with 38 wt % butene	104
H52 (D52)	model EB copolymer with 52 wt % butene	85
H66A (D66A)	model EB copolymer with 66 wt % butene	114
H66B	model EB copolymer with 66 wt % butene	125
H78 (D78)	model EB copolymer with 78 wt % butene	73
H88 (D88)	model EB copolymer with 88 wt % butene	91
H90 (D90)	model EB copolymer with 90 wt % butene	28
H97B (D97B)	model EB copolymer with 97 wt % butene	48.4
HPEP (DPEP)	model alternating copolymer of ethylene and propylene with ~60 wt % propylene	59.9
EP-JBG11	commercial ethylene-propylene copolymer with 57 wt % propylene from Exxon	151
HPEB (DPEB)	model alternating copolymer of ethylene and butene with ~66 wt % butene	46.3
H50SPI (D50SPI)	model statistical copolymer derived from polyisoprene (50% 1,4 and 50% 3,4)	104
H34SPI (D75SPI)	model statistical copolymer derived from polyisoprene (75% 3,4 and 25% 1,2)	73
HPPB (DPPB)	model head-to-tail polypropylene	59.2
HhhPPA (DhhPPA)	model head-to-head polypropylene	27.5
HhhPPC (DhhPPC)	model head-to-head polypropylene	172.3

Table 2. Visual Observations and Cloud Point Determinations

sample	ϕ_{PIB}	observations
PIBB/D97B	0.49 ₈	phase separated 25–100 °C and formed droplets
PIBB/D90	0.47 ₉	phase separated 25–120 °C and formed droplets
PIBB/D78	0.55 ₀	miscible at 25 °C, phase separation at 85 ± 5 °C, studied by SANS
PIBC/D78	0.46 ₇	miscible at 25 °C, phase separation at 75 ± 5 °C
PIBA/D66A	0.50 ₃	miscible at 25 °C, phase separation at 105 ± 5 °C
PIBB/D66A	0.51 ₂	miscible at 25 °C, phase separation at 100 ± 5 °C, studied by SANS
PIBC/D66A	0.49 ₆	miscible at 25 °C, phase separation at 95 ± 5 °C, studied by SANS
PIBB/H66A	0.49 ₈	miscible at 25 °C, phase separation at 100 ± 5 °C
PIBD/D66A	0.52 ₁	miscible at 25 °C, phase separation at 90 ± 5 °C
PIBB/D52	0.49 ₉	miscible at 25 °C, phase separation at 95 ± 5 °C, studied by SANS
PIBD/D52	0.49 ₀	miscible at 25 °C, phase separation at 90 ± 5 °C
PIBA/D38	0.50 ₂	phase separated at 25 °C, no droplets, remained phase separated at elevated temperatures; uncertain at 25 °C because $T_m = 40$ °C for D38
PIBA/DPEB	0.45 ₄	miscible at 25 °C, phase separation at 50 ± 5 °C, mixture cleared when cooled back to 25 °C
PIBB/DPEP	0.50 ₉	phase separated at 25 °C, no droplets, macrodomain formation upon heating
PIBA/DPEP	0.80 ₂	miscible at 25 °C, phase separation at 45 ± 5 °C, cleared when cooled back to 25 °C
PIBC/EP-JBG11	0.05 ₀	miscible at 25 °C phase separation at 50 ± 5 °C, cleared when cooled back to 25 °C
PIBD/EP-JBG11	0.10	miscible at 25 °C, phase separation at 50 ± 5 °C, cleared after a long time when cooled back to 25 °C
PIBB/DPPB	0.50 ₇	phase separated up to at least 100 °C, formed droplets
PIBB/DhhPPA	0.47 ₅	miscible at 25 °C, phase separation at 190 ± 10 °C, studied by SANS
PIBB/HhhPPA	0.51 ₀	miscible at 25 °C, phase separation at 185 ± 10 °C
PIBC/DhhPPC	0.48 ₉	miscible at 25 °C, phase separation at 175 ± 10 °C
PIBC/D50SPI	0.52 ₁	borderline miscibility at 25 °C, definitely phase-separated at 40 °C, no macrodomain formation
PIBA/D75SP	0.50 ₃	phase separated at 25 °C, formed droplets that increased in size with heating

52 wt % of the butene structure while D52 is the partially deuterated version, HPEP is a predominantly alternating ethylene-propylene copolymer, HPEB is a predominantly alternating ethylene-butene copolymer, HPP is a conventional (head-to-tail) polypropylene, HhhPP is head-to-head polypropylene, and H50SPI and H75SPI are hydrogenated versions of polyisoprenes with enhanced 3,4 and 1,2 enchainments. For all these materials, $M_w/M_n \leq 1.07$. We also used a commercial ethylene-propylene copolymer from Exxon, EP-JBG11, which contains 57 wt % propylene.

All components are atactic with glass transition below room temperature. All are clear noncrystalline liquids at room temperature except H38 ($T_m = 42$ °C). They were dissolved and filtered (0.22 μ m Anodisc) prior to use. Blends were prepared by mixing known weights of the components in dilute solution and evaporating to dryness. As in past work,¹⁻⁸ blend compositions are routinely expressed as nominal volume fractions: $\phi_i = (w_i/\rho_i)/(w_1/\rho_1 + w_2/\rho_2)$, where the w_i and ρ_i are weight fractions and pure component densities.

The SANS measurements were conducted at the NIST Cold Neutron Research Facility in Gaithersburg, MD.¹³ Experimental procedures and the analysis of data to obtain χ were generally carried out as described in previous work.¹ The light scattering procedures to determine cloud points for the blends were also described earlier.¹ Densities were measured at 23 °C with a density-gradient column. Glass transition tempera-

ture T_g was determined with a Seiko calorimeter (Model SSC5200H with subambient capability) at a heating rate of 10 °C/min. Phase boundaries were determined with the same instrument by annealing blends at various elevated temperatures for 1 h, followed by rapid quenching to -105 °C and subsequent T_g scanning at 10 °C/min. The presence of two distinct glass transitions was taken to indicate phase separation at the annealing temperature. The PVT data were obtained with a Gnomix instrument and provided through the courtesy of Drs. G. T. Dee and D. J. Walsh, DuPont Central Research and Development.¹⁴

Results

A. Miscibility Survey and Cloud Point Determinations. Table 2 lists the PIB blends that were examined initially. Many were obviously phase-separated at room temperature and remained so at elevated temperatures. These were not studied further. The other blends were single phase at room temperature but underwent phase separation at elevated temperatures. None remained single phase above 190 °C, and all reverted eventually to single phase upon cooling back to room temperature. Their cloud points were determined by increasing the temperature at a rate of 4 °C/h

while recording the scattering intensity. At phase separation the intensity rose rapidly and then decreased sharply. The temperature at the onset of the rise was taken to be the phase separation temperature (Table 2). The transition itself was reversible, although the cooling transition was found to be unreliable: the dynamics of reversion were rather slow, and the results were found to depend on the history of prior superheating. The results for heating were reproducible to ± 1 °C, but the absolute accuracy for most experiments is more nearly ± 5 °C.

The following conclusions were drawn from these studies.

(1) All the PIB blends surveyed that are miscible at room temperature exhibit phase separation at elevated temperatures and thus LCST behavior.

(2) Cloud point results for the PIBB/H66A and PIBB/D66A blends as well as the PIBB/HhhPPA and PIBB/DhhPPA blends suggest that deuterium labeling has a negligible effect on phase behavior in PIB blends. This contrasts strongly with results of our previous studies of model polyolefin blends, which showed large effects on the critical temperature T_c as a result of deuterium substitution alone.^{2,3,5}

(3) PIB is miscible at room temperature with a modest range of model polyolefin microstructures. Thus, PIB is miscible with D52, D66, and D78 (ethylene–butene copolymers with 52–78 wt % butene) and also with DPEP (borderline), DPEB, and DhhPP. PIB is immiscible with D38, D90, and D97 as well as DPP, D50SPI, and D75SPI. Based on previous assignments of the solubility parameter, $(\delta - \delta_{ref})_{SANS}$, for these various microstructures,^{6–8} PIB would appear to have a room-temperature window of miscibility for polyolefins with solubility parameters that extend roughly from δ_{50} to δ_{80} , encompassing the 52, 66, 78, PEP, PEB, and hhPP microstructures and excluding 38, 90, 97, PP, 50SPI, and 75SPI.

(4) The results for blends of PIB with D66A indicate that phase separation temperature is remarkably insensitive to component molecular weight. Thus, M_w for PIBA and PIBC differs by a factor of 4, yet the phase separation temperature shifts by only 10 °C. The blends of PIB with hhPP behave similarly. In other polyolefin blends, T_c can shift by as much as 80 °C when the molecular weight of a component is changed by only a factor of 2.¹

(5) DPEB and D66A have the same weight fractions of butene units but differ in sequencing (alternating *vs* statistical), and both are miscible with PIB at 25 °C. However, the phase separation temperatures are significantly different, being higher for PIBA/H66A by ~ 50 °C despite a much larger M_w for H66A than DPEB. On the other hand, DPEP and EP-JBG11 have nearly the same weight fraction of propylene units and also differ mainly in sequencing, yet their blends with PIB appear to have rather similar (borderline) miscibility characteristics. The distinction between head-to-head and head-to-tail configuration, however, has a major effect on miscibility with PIB. Thus, PIB/hhPP blends have the highest phase separation temperatures of all the systems investigated, yet PIB/PP blends are immiscible even at room temperature.

(6) Model PIB and commercial PIB are indistinguishable in miscibility behavior as shown by the similarity of results for blends of PIBB, PIBC, and PIBD with the 52 and 66 species.

Table 3. Interaction Parameters Determined by SANS

blend	$\chi \times 10^4$			
	27 °C	51 °C	83 °C	167 °C
PIBB/D52 ($\phi_{PIB} = 0.49_9$)	-18.2	-2.5	2P ^a	2P
PIBB/D66A ($\phi_{PIB} = 0.51_2$)	-45.9	-23.1	-2.3	2P
PIBC/D66A ($\phi_{PIB} = 0.49_6$)	-43.7	-21.5	-1.0	2P
PIBB/D78 ($\phi_{PIB} = 0.46_7$)	-21.4	-8.7	+3.8	2P
PIBB/DhhPPA ($\phi_{PIB} = 0.47_5$)	-101.	-72.	-37.4	+10.1

^a 2P = two liquid phases.

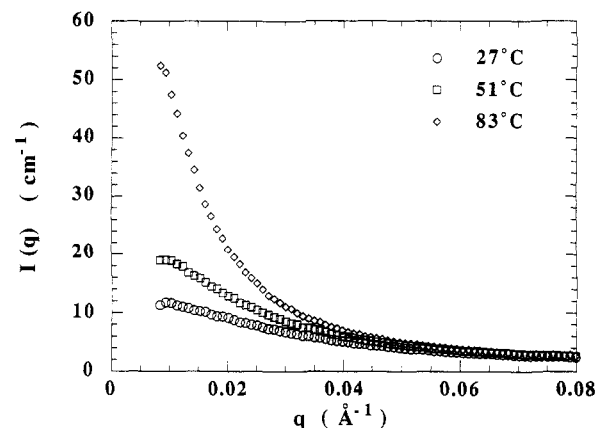


Figure 1. Angular dependence of total SANS intensity for PIBC/D66A at various temperatures.

B. Small-Angle Neutron Scattering Results.

Five blends that are miscible at room temperature—PIBB/D52, PIBB/D66A, PIBC/D66A, PIBB/D78, and PIBB/DhhPPA—were studied in the single-phase region by SANS. The dependence of scattering form factor $P(q)$ and radius of gyration R_g on temperature was determined for the model polyolefin components by matched-pair experiments.¹ Only hydrogenous versions of PIB were available, so we calculated $P(q)$ for PIBB and PIBC with the Debye equation for random coils

$$P(q) = \frac{2}{u^2} [e^{-u} - 1 + u] \quad (1)$$

$$u = R_g^2 q^2$$

using $R_g(M, T)$ for PIB from Hayashi et al.¹⁵ and a modified version of eq 1 to account for their modest polydispersities.¹⁶ The incoherent background was subtracted from the total scattering intensity $I(q)$ for the blends and converted to the static structure factor $S(q)$ as described previously.¹ The random phase approximation and the Flory–Huggins equation were then applied to obtain the interaction parameter χ , defined with respect to the reference volume $v_0 \equiv (v_1 v_2)^{1/2}$, v_1 and v_2 being the component volumes per mer at the temperature of the measurements.¹ The results are given in Table 3.

The total scattering intensity in absolute units for the PIBC/D66A blend at various temperatures is shown in Figure 1. The scattering profile at the lowest temperature depends only weakly on q . Concentration fluctuations are suppressed, indicating a strong net attraction between the components. The intensities at low q increase rapidly with increasing temperature, corresponding to a weakening attraction and finally repulsion as the phase separation (95 ± 5 °C for this blend) is approached. The results for all five blends, given in Table 3, show the same behavior. The values of χ are

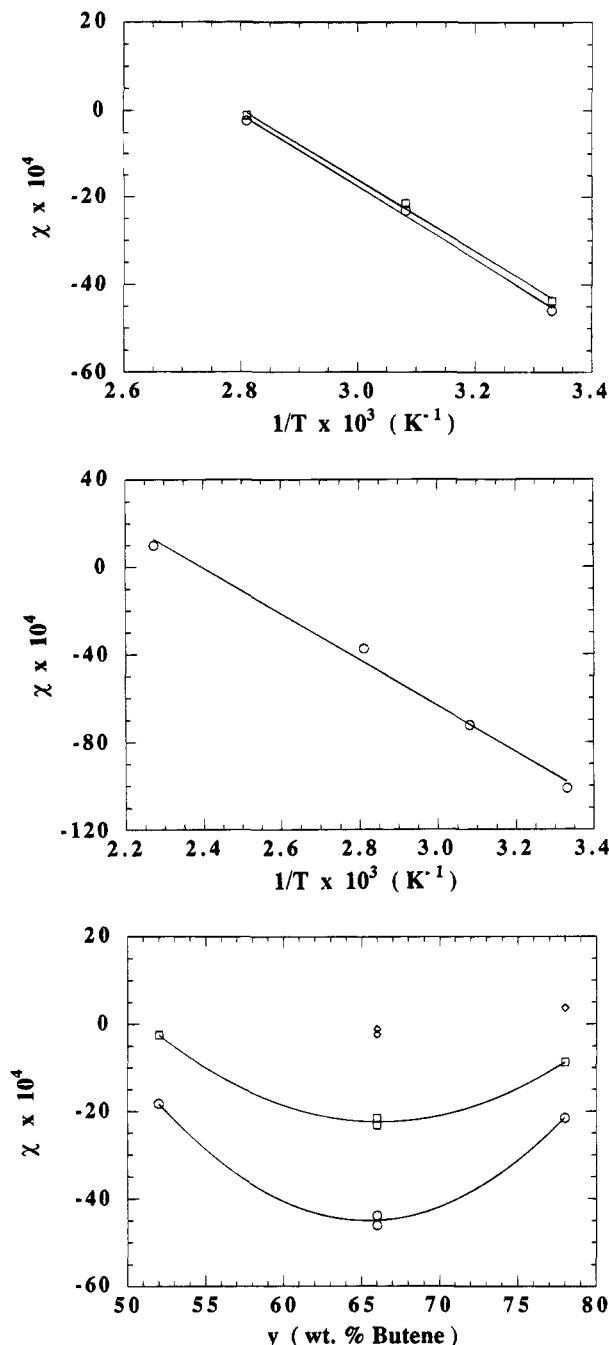


Figure 2. (a, Top) Temperature dependence of the interaction parameter for PIBB/D66A and PIBC/D66A blends. (b, Middle) Temperature dependence of the interaction parameter for PIBB/DhhPPA blends. (c, Bottom) Dependence of interaction parameter on component composition for blends of PIB with D52, D66A, and D78. The symbols indicate measurement temperatures of 27 (○), 51 (□), and 83 °C (◇).

large and negative at 27 °C but move rapidly toward zero and then on to positive values at phase separation at higher temperatures.

The chain dimensions for PIB extracted independently from the blend scattering at intermediate q are in good agreement with the prediction.¹⁵ Thus $R_g(M, T)$ appears to be insensitive to the strength of the blend interactions, as we have found in previous studies with polyolefin blends.³

The interaction parameter itself is insensitive to component molecular weight, as judged by the results shown in Figure 2a for PIBB/D66A and PIBC/D66A. This observation is consistent with previous results for

Table 4. Density and Thermal Transition Properties for H66B/PIBE Blends

sample	wt frac PIB	vol frac PIB	density ρ (g/cm ³)	T_g (°C)	ΔT_g (°C)	$(v_E/v_0)_{\text{obs}} \times 10^4$	$(v_E/v_0)_{\text{PVT}} \times 10^4$
H66B	0.0	0.0	0.8617	-52.8	5.8	0	0
#1	0.097	0.092	0.8671	-53.7	7.5	+3	-2
#2	0.179	0.171	0.8713	-54.7	8.4	+2	-3
#3	0.301	0.288	0.8777	-55.1	10.3	+1	-4
#4	0.330	0.317	0.8792	-56.9	11.7	0	-4
#5	0.409	0.395	0.8833	-58.7	12.8	-1	-5
#6	0.500	0.485	0.8881	-60.4	14.2	-2	-5
#7	0.564	0.549	0.8916	-61.0	12.6	+1	-5
#8	0.682	0.669	0.8978	-63.5	9.8	-1	-4
#9	0.789	0.779	0.9032	-64.3	8.8	-3	-3
#10	0.916	0.911	0.9099	-64.6	6.7	-4	-1
PIBE	1.0	1.0	0.9147	-63.9	5.7	0	0

blends of saturated hydrocarbon polymers.⁸ Also, the temperature dependence of χ for all five PIB blends follows the conventional $A/T + B$ form reasonably well. The data for PIBB/DhhPPA blends, which cover the widest span of temperatures, are shown in Figure 2b. Finally, the trends in χ with ethylene-butene copolymer composition (HPIB/D52, HPIB/D66A, HPIB/D78) are shown in Figure 2c. The results suggest the existence of a miscibility window for PIB with a range of ethylene-butene microstructures, centered near 65 wt % butene, as also indicated by the cloud point studies.

The temperatures obtained by extrapolating $\chi(T)$ to the respective critical interaction parameter for the blend

$$\chi_c = \frac{v_0}{2} [(\rho_1/M_1)^{1/2} + (\rho_2/M_2)^{1/2}]^{-2} \quad (\text{Flory-Huggins}) \quad (2)$$

agree reasonably well with the observed cloud point temperatures (Table 2). Thus, the insensitivity of cloud point temperature to component molecular weight, remarked upon earlier, appears to be mainly a consequence of the extraordinarily rapid change in interaction strength with temperature in the PIB blends.

C. Glass Transition and Volume Change on Mixing for PIBE/H66B Blends. Ten blends of PIBE and H66B were prepared by mixing in dilute solution, filtering, precipitating, and exhaustive drying. Samples of the pure components were prepared identically. As expected from the results in Table 2 for PIB/66 blends, all were single phase at 25 °C and showed only one glass transition peak by calorimetry. The values of T_g and transition width ΔT_g were essentially identical in repeat runs, and neither was changed by many hours of prior annealing at 55 or at 75 °C. Both T_g and ΔT_g are recorded in Table 4. The variation in T_g with blend composition is shown in Figure 3. The line is the Fox-Flory prediction, $(T_g)_{\text{blend}}^{-1} = \phi_1(T_g)_1^{-1} + \phi_2(T_g)_2^{-1}$.

The densities ρ of the same blends and pure components, ρ_1 and ρ_2 , were determined at 23 °C using at least four specimens of each. To minimize systematic errors, all measurements were made on the same day and in the same density-gradient column. Agreement among the four specimens was better than ± 1 mm in column location (better than ± 0.00015 g/cm³ in density). The results are recorded in Table 4. The fractional volume change on mixing was calculated from the density of the blend and the densities and weight fractions of the blend components:

$$\left(\frac{v_E}{v_0}\right)_{\text{obs}} = \left(\frac{1}{\rho} - \frac{w_1}{\rho_1} - \frac{w_2}{\rho_2}\right) \left(\frac{w_1}{\rho_1} + \frac{w_2}{\rho_2}\right) \quad (3)$$

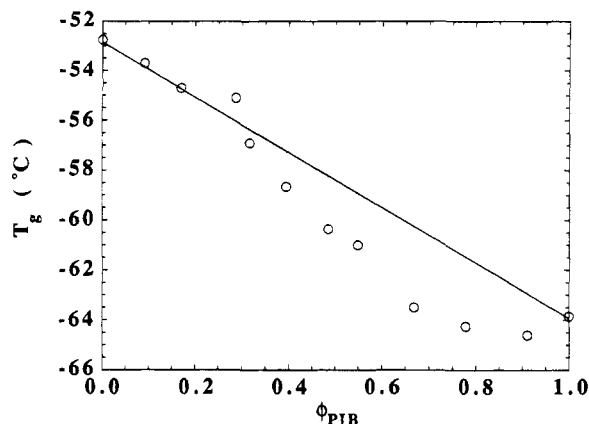


Figure 3. Glass transition temperature as a function of blend composition for PIBE/H66B. The curve is the Fox-Flory prediction.

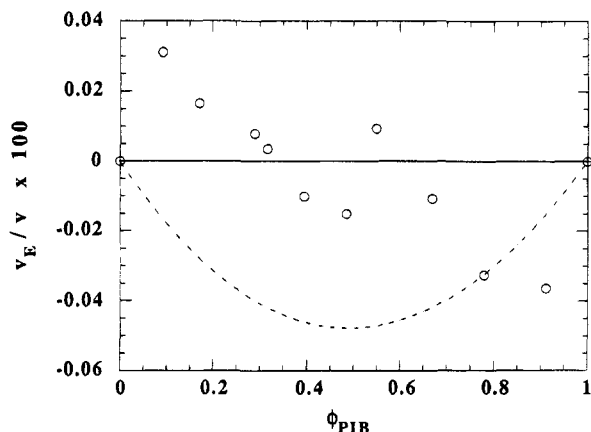


Figure 4. Fractional volume change on mixing as a function of blend composition for PIBE/H66B. The dashed curve is a prediction based on pure component PVT properties.

The values of $(v_E/v_0)_{obs}$ are recorded in Table 4 and shown as a function of blend composition in Figure 4.

The combination of results in Figures 3 and 4 is somewhat counterintuitive. Thus, for example, the volume decreases with mixing in PIB-rich blends, presumably reducing the free volume and thereby increasing T_g , yet T_g actually decreases slightly in this region ($\phi_{PIB} = 0.78$ and 0.91). Also, the volume increases with mixing in the H66-rich blends, presumably increasing the free volume and thereby lowering T_g , yet T_g in that same region obeys the Fox-Flory relation rather well.

The difference in pure component T_g is only 11 °C, and the transition width becomes comparable to that difference in the composition midrange (Table 4). Moreover, the volume changes themselves are very small, being less than 0.04% in magnitude and thus barely within the resolution of careful density-gradient column methods. The observations shown in Figures 3 and 4 are, nevertheless, still outside the errors, but unfortunately their fundamental significance is still unknown. Some theoretical estimates of v_E/v_0 based on the pure component PVT properties were made as described in the Appendix. Those results are shown in the last column of Table 4. The order of magnitude is consistent with $(v_E/v_0)_{obs}$, but the calculated values are negative at all compositions. Unfortunately, even the sign of those predictions is uncertain, owing to the extreme sensitivity of $(v_E/v_0)_{PVT}$ to the fitting parameters (see Appendix).

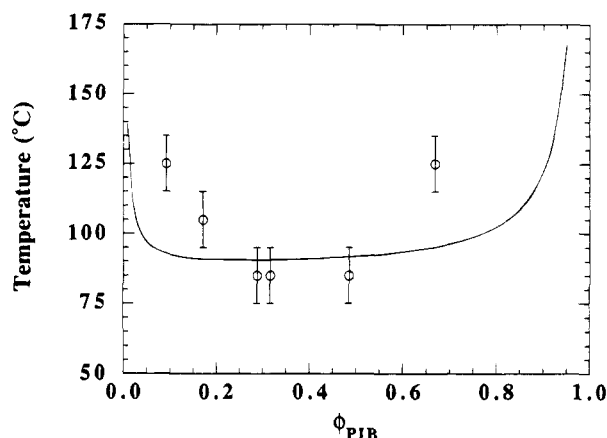


Figure 5. Phase diagram for PIBE/H66B blends based on a quenching-calorimetry procedure. The solid curve is the spinodal diagram calculated with the Flory-Huggins theory and $\chi(T)$ for PIB/D66A blends.

D. Phase Diagram for PIBE/H66B Blends. Several of the PIBE/H66A blends used in the studies of glass transition temperature and density were annealed at various elevated temperatures, quenched, and then scanned by DSC as described in the Experimental Section. Quenched blends which showed a single T_g were assumed to be single phase at the annealing temperature; those with two T_g 's were deemed to be two phase. The results are shown in Figure 5 as a function of blend composition. The bars for each composition indicate the highest annealing temperature with a single T_g and the lowest annealing temperature with two T_g 's. The points are the average of these two temperatures; the curve is the spinodal curve calculated with the Flory-Huggins theory and χ vs T as obtained by SANS (Figure 2a).

The shape of the experimental phase diagram indicates classical LCST behavior, with a critical composition that appears to be consistent with $(\phi_{PIB})_c = 0.27$, a value estimated from the component densities and molecular weights:

$$(\phi_1)_c = \frac{(M_1/\rho_1)^{1/2}}{(M_1/\rho_1)^{1/2} + (M_2/\rho_2)^{1/2}} \quad (\text{Flory-Huggins}) \quad (4)$$

The phase boundary temperature is rather insensitive to blend composition, ranging only about 20 °C from $\phi_{PIB} \sim 0.09$ to $\phi_{PIB} \sim 0.69$. Like the insensitivity of T_c to component molecular weights described earlier, the flatness of the experimental phase boundary is probably caused by the large temperature dependence of interaction strength in PIB/66 blends (Figure 2a). The discrepancy between experimental results and predicted spinodal in Figure 5 might indicate a significant dependence of χ on blend composition, which we have not investigated.

E. PVT Properties of PIB. In earlier work with other blends of model polyolefins, for which the interaction parameters from SANS were generally positive, we found that the majority of results for the composition midrange ($\phi_1 \approx \phi_2$) could be organized rather well through the Hildebrand equation:

$$\chi(T) = \frac{v_0}{k_B T} (\delta_2 - \delta_1)^2 \quad (5)$$

in which δ_1 and δ_2 are temperature-dependent solubility

Table 5. PVT Parameters for PIB and PEP

<i>T</i> (°C)	α (K ⁻¹) × 10 ⁴		β (MPa ⁻¹) × 10 ⁴		δ_{PVT} (MPa ^{1/2})	
	PIB	PEP	PIB	PEP	PIB	PEP
27	5.5 ₂	6.6 ₀	4.8 ₀	5.8 ₂	18.5 ₈	18.4 ₆
51	5.7 ₂	6.7 ₈	5.5 ₂	6.7 ₄	18.3 ₃	18.0 ₆
83	5.5 ₃	6.6 ₉	6.2 ₉	7.8 ₇	17.6 ₈	17.3 ₉
121	5.6 ₈	6.8 ₈	7.4 ₁	9.3 ₀	17.3 ₈	17.0 ₇
167	6.0 ₈	7.3 ₃	8.8 ₅	11.5 ₀	17.3 ₈	16.7 ₄

Table 6. Values of Relative Solubility Parameter Based on PVT Properties for Various Saturated Hydrocarbon Polymers

species	$(\delta - \delta_{ref})_{PVT}$ (MPa ^{1/2}) at temperature <i>T</i> (°C)				
	27	51	83	121	167
H97	0.0 ₀	0.0 ₀	0.0 ₀	0.0 ₀	0.0 ₀
HPP	0.2 ₀	0.2 ₆	0.1 ₇	0.0 ₉	0.0 ₁
H66	0.5 ₉	0.6 ₈	0.9 ₂	0.8 ₄	0.8 ₀
HhhPP	0.6 ₃	0.6 ₉	0.7 ₇	0.8 ₃	0.8 ₂
H52	0.7 ₆	0.8 ₀	0.7 ₅	0.8 ₀	0.7 ₉
HPEB	0.9 ₈	0.6 ₉	0.8 ₂	0.7 ₅	0.8 ₂
HPEP	1.2 ₆	1.1 ₇	1.0 ₁	1.2 ₃	0.8 ₇
H32		1.1 ₂	1.3 ₄	1.1 ₅	1.3 ₆
PIB	1.3 ₉	1.4 ₄	1.3 ₀	1.5 ₄	1.5 ₁
H08				1.6 ₁	1.5 ₈

parameters for the blend components. Empirical values relative to a reference species H97, $(\delta - \delta_{ref})_{SANS}$, were assigned to the various species and confirmed through a detailed system of internal consistency tests for their blends.⁶⁻⁸ Blends for which the observed interactions were consistent with eq 5 and these $(\delta - \delta_{ref})_{SANS}$ assignments were said to mix regularly. The results for some blends departed from this pattern, and the interactions for those blends were expressed in terms of an extra interaction density coefficient, quantifying the extent of their irregularity:

$$X_E = \frac{k_B T \chi}{v_0} - (\delta_2 - \delta_1)^2 \quad (6)$$

where $\delta_2 - \delta_1 = (\delta_2 - \delta_{ref})_{SANS} - (\delta_1 - \delta_{ref})_{SANS}$.

None of the miscible PIB blends investigated by SANS mix regularly of course, since eq 5 requires, at minimum, that χ be positive. Thus, confirmed values of $(\delta - \delta_{ref})_{SANS}$ cannot be determined for PIB, at least with the blend data presented here. On the other hand, our previous work has shown that the SANS-based solubility parameters parallel rather closely the values estimated from pure component PVT data.⁶⁻⁸ We used the expression based on the square root of internal pressure to define^{17,18}

$$\delta_{PVT} = (T\alpha/\beta)^{1/2} \quad (7)$$

where α is the thermal expansion coefficient and β the isothermal compressibility. The values of $\alpha(T)$ and $\beta(T)$ for PIB at ambient pressures were obtained with previously published data,¹⁴ and they agree well with results for PIB reported by others.¹⁹ They are recorded in Table 5 along with the values of $\delta_{PVT}(T)$ obtained with eq 7. Values of $\delta_{PVT}(T)$ are already available for the reference species H97 and several other model polyolefins.⁶⁻⁸ For comparison purposes, the values of α , β , and δ_{PVT} for PEP, which are typical for the model polyolefins, are also listed in Table 5.

The values of $(\delta - \delta_{ref})_{PVT}$ for several polyolefins are compared with those for PIB in Table 6. These data would seem to suggest that the solubility parameter for PIB lies between the values for H08 and H32, cor-

Table 7. Extra Mixing Energy Coefficient for PIB Blends

blend	X_E (MPa)			
	27 °C	51 °C	83 °C	167 °C
PIB/D52	-0.47	-0.41		
PIB/D66	-0.82	-0.67	-0.53	
PIB/D78	-1.08	-1.04	-1.00	
PIB/DhhPP	-0.91	-0.67	-0.56	-0.43

responding to an ethylene-butene copolymer with perhaps 20 wt % butene. Curiously, this location, $\delta_{PIB} \sim \delta_{20}$, is rather far removed from the PIB miscibility window with other polyolefins, roughly δ_{50} to δ_{80} as identified in part A of the Results.

We have no explanation for this displacement, nor indeed for the very existence of strong attractions (negative χ) in PIB blends, although it is perhaps worth noting that PIB is somewhat anomalous in many respects among saturated hydrocarbon polymers. Thus, its density, $\rho = 0.915$ g/cm³ at 23 °C, is distinctly larger than those for the other polyolefin liquids, which range from 0.85 to 0.87 g/cm³. Also, both thermal expansion coefficient and isothermal compressibility are distinctly smaller for PIB, as shown by the comparison of α and β with the more typical values for PEP in Table 5. Evidently, PIB molecules are arranged more compactly in the liquid state and their intermolecular forces resist more strongly the perturbing effects of pressure and temperature, but why this should be is unknown. The ratio α/β , which governs δ_{PVT} through eq 7, turns out to be similar for PIB and the other polyolefins, but the fact remains that the interactions between their chains must be very different. How this leads to strong stabilization of the single phase in certain PIB blends and why that stabilization decreases rapidly with increasing temperature are major mysteries.

We have found other examples of strong stabilization in earlier work,⁸ although none that actually led to negative values of χ . Values of X_E (eq 6) as large as -0.40 MPa (J/cm³) were found for PP/PEP blends and -0.25 MPa for PP/hhPP blends. Lacking values of $(\delta_{PIB} - \delta_{ref})_{SANS}$, we used those based on PVT measurements (Table 6) to estimate X_E with eq 6 and the SANS data (Table 3) for PIB blends. Those values are listed in Table 7. The largest is -1.0 MPa, clearly beyond the PP/PEP and PP/hhPP stabilizations but not outlandishly so.

We will consider these and other examples of irregular mixing in a forthcoming paper that deals more completely with pure component PVT properties.²⁰

Concluding Remarks

We have shown that PIB is miscible at room temperature with a modest range of polyolefin species. All such PIB blends exhibit LCST behavior with phase separation temperatures from 40 to 190 °C, depending on the second species. The phase separation temperature is also insensitive to both component molecular weight and blend composition. At room temperature the values of χ for these blends are large and negative, but they diminish in magnitude rapidly with increasing temperature, eventually crossing zero and becoming positive just prior to phase separation. The interaction parameters themselves appear to be independent of component molecular weight, as expected from theory and found for other polyolefin blends. We have not studied the dependence of χ on composition. Nevertheless, the strong temperature dependence χ alone explains at least qualitatively, through the Flory-

Huggins formulas, the observed insensitivity of phase separation temperature to both molecular weight and composition in PIB blends.

We have noted many anomalies in the properties of PIB relative to those of other saturated hydrocarbon polymers—larger density, smaller thermal expansion coefficient, and smaller isothermal compressibility. We have also reported density and T_g anomalies in PIB blends. An additional anomaly is evident from the difference between the apparent solubility parameter for PIB and the location of its miscibility window with polyolefins. Thus, δ_{PIB} from PVT measurements would appear to be near that for the H20 microstructure, i.e., δ_{20} , but the polyolefins that are miscible with PIB have solubility parameter in the interval from δ_{50} to δ_{80} , which of course would suggest $\delta_{PIB} \approx \delta_{65}$ by the conventional criterion.

These peculiarities of PIB and its blends are perhaps related to the remarkable feature of large negative values for χ , i.e., strong net attraction between components, in blends of saturated hydrocarbon polymers. The species contain neither polar groups nor other moieties with the potential to form specific interactions, such as hydrogen bonding or charge-transfer complexation. The intermolecular energies of saturated hydrocarbon liquids originate from induced-dipole interactions, and these are expected to produce only a net repulsion between components, or positive χ , in liquid mixtures. Moreover, equation-of-state contributions can only serve to enhance these repulsions.²¹ The only possibility is a local packing contribution, strengthening the attractions and specific to the component pair. We offer this "explanation" in the absence of other alternatives.

Acknowledgment. Financial support for this work (W.W.G. and R.K.) was provided by grants from the National Science Foundation to Princeton University (DMR89-05187 and DMR93-10762). We are grateful to Dave Walsh and Greg Dee for their generosity in providing the PVT data, to Joe Sissano for the polybutadiene precursor of H66B, to Nitash Balsara for early discussions of the work, and to Glenn Reichart for providing some of the SANS data. Recent conversations with Ken Schweizer and Sanat Kumar were also very helpful.

Appendix. Estimation of Excess Volume of Mixing

The Flory–Huggins theory makes no provision for volume changes in mixing. Here we use the Flory–Orwoll–Vrij (FOV) cell model to estimate v_E/v_0 for PIB/H66 blends following the procedures prescribed in ref 9. The FOV equation of state takes the corresponding states form

$$\frac{\tilde{P}\tilde{v}}{\tilde{T}} = \frac{\tilde{v}^{1/3}}{\tilde{v}^{1/3} - 1} - \frac{1}{\tilde{v}\tilde{T}} \quad (1A)$$

in which $\tilde{P} = P/P^*$, $\tilde{T} = T/T^*$, and $\tilde{v} = v/v^*$; P , T , and $v(P, T)$ are the pressure, temperature, and specific volume; and P^* , T^* , and v^* are fitting parameters that characterize the liquid.

The FOV combining rules for binary mixtures take the form

$$P^* = \phi_1^* P_1^* + \phi_2^* P_2^* \quad (2A)$$

Table 8. FOV Fitting Parameters for PIB and H66

data set	polymer	P^* (MPa)	T^* (K)	v^* (g/cm ³)
low-temperature block	PIB	427	7254	0.9513
low-temperature block	H66	471	6201	0.9708
high-temperature block	PIB	469	7693	0.9558
high-temperature block	H66	447	6797	0.9895
low-temperature block (adjusted)	PIB	502	6851	0.9513
low-temperature block (adjusted)	H66	471	6201	0.9708

$$\frac{1}{T^*} = \frac{\phi_1^* P_1^*/T_1^* + \phi_2^* P_2^*/T_2^*}{\phi_1^* P_1^* + \phi_2^* P_2^*} \quad (3A)$$

in which the P_i^* and T_i^* are pure component values and the ϕ_i^* are the "hard core" volume fractions of the components in the mixture: $\phi_i^* = w_i v_i^*/(w_1 v_1^* + w_2 v_2^*)$, the w_i being the component weight fractions. (We have omitted the interaction term, which we, as well as others,¹¹ have found to make a negligible contribution to $(v_E/v_0)_{PVT}$ for blends.)

At zero pressure the left side of eq 1a vanishes, leaving

$$\frac{\tilde{v}^{1/3} - 1}{\tilde{v}^{4/3}} = \frac{T}{T^*} \quad (4A)$$

which combines with eq 3a to give

$$\frac{\tilde{v}^{1/3} - 1}{\tilde{v}^{4/3}} = T \frac{\phi_1^* P_1^*/T_1^* + \phi_2^* P_2^*/T_2^*}{\phi_1^* P_1^* + \phi_2^* P_2^*} \quad (5A)$$

The reduced volume \tilde{v} for blends can thus be calculated from pure component data and blend composition and then used to evaluate the fractional change in volume with mixing as a function of composition:

$$(v_E/v_0)_{PVT} = \frac{\tilde{v} - (\phi_1^* \tilde{v}_1 + \phi_2^* \tilde{v}_2)}{\phi_1^* \tilde{v}_1 + \phi_2^* \tilde{v}_2} \quad (6A)$$

Values of P^* , T^* , and v^* for PIB and H66 were obtained by fitting their PVT data to eq 1A.¹⁴

There are systematic errors of two kinds that must be considered. First, the FOV equation does not fit the full PVT data set precisely, a defect it shares with all other equation-of-state models. Two sets of P^* , T^* , and v^* were established, one covering the low-temperature range ($50 \leq T \leq 150$ °C; $10 \leq P \leq 200$ MPa), the other covering the high-temperature range ($150 \leq T \leq 250$ °C; $10 \leq P \leq 200$ MPa). Second, the data for PIB and H66 were measured with different instruments and experimental protocols, and we have found small systematic differences between results for the same polymer in these circumstances.²⁰ A third set of fitting parameters was obtained for the low-temperature range by what we believe to be reasonable adjustments to compensate for the instrument and protocol differences. The results are listed in Table 8.

Rather different values of $(v_E/v_0)_{PVT}$ were obtained through eqs 5A and 6A with the three sets of fitting parameters. The predictions are extremely sensitive to the fitting choice. Those from the low-temperature block were positive, while those from the high-temperature block and adjusted low-temperature block were negative. All were symmetric around $\phi = 0.50$ and obeyed with remarkable fidelity the classical $\phi(1 - \phi)$ dependence, but the values at $\phi = 0.50$ were +0.033, −0.047, and −0.051%, respectively. Those obtained

from the adjusted parameter set are listed in Table 4 and shown by the dashed line in Figure 4. The magnitudes of $(v_E/v_0)_{PVT}$ in all cases are in the observed range, $\pm 0.04\%$, but the important point is that the composition dependence for all parameter sets bears no resemblance at all to the observed behavior. To our knowledge, the only other example that even faintly resembles our $(v_E/v_0)_{obs}$ results in figure 4 is the benzene-perdeuteriobenzene system.²² Although we have no proof, our experience with calculations of $(V_E/v_0)_{PVT}$ for other blends, where the same instrument and protocols were used to obtain the PVT data, suggests that the $\phi(1 - \phi)$ form of composition dependence is always predicted by equation-of-state models when the volume change on mixing is very small.

References and Notes

- (1) Balsara, N. P.; Fetters, L. J.; Hadjichristidis, N.; Lohse, D. J.; Han, C. C.; Graessley, W. W.; Krishnamoorti, R. *Macromolecules* **1992**, *25*, 6137.
- (2) Graessley, W. W.; Krishnamoorti, R.; Balsara, N. P.; Fetters, L. J.; Schulz, D. N.; Sissano, J. A. *Macromolecules* **1993**, *26*, 1137.
- (3) Krishnamoorti, R.; Graessley, W. W.; Balsara, N. P.; Lohse, D. J. *J. Chem. Phys.* **1994**, *100*, 3894.
- (4) Balsara, N. P.; Lohse, D. J.; Graessley, W. W.; Krishnamoorti, R. *J. Chem. Phys.* **1994**, *100*, 3905.
- (5) Graessley, W. W.; Krishnamoorti, R.; Balsara, N. P.; Fetters, L. J.; Lohse, D. J.; Schulz, D. N.; Sissano, J. A. *Macromolecules* **1994**, *27*, 2574.
- (6) Krishnamoorti, R.; Graessley, W. W.; Balsara, N. P.; Lohse, D. J. *Macromolecules* **1994**, *27*, 3073.
- (7) Graessley, W. W.; Krishnamoorti, R.; Balsara, N. P.; Butera, R. J.; Fetters, L. J.; Lohse, D. J.; Schulz, D. N.; Sissano, J. A. *Macromolecules* **1994**, *27*, 3896.
- (8) Graessley, W. W.; Krishnamoorti, R.; Reichart, G. C.; Balsara, N. P.; Fetters, L. J.; Lohse, D. J., *Macromolecules*, in press.
- (9) Flory, P. J.; Ellenson, J. L.; Eichinger, B. E. *Macromolecules* **1968**, *1*, 279.
- (10) (a) Rowlinson, J. S.; Freeman, P. I. *Polymer* **1960**, *1*, 20. (b) Patterson, D.; Delmas, G.; Somcynsky, T. *Polymer* **1967**, *8*, 503. Bardin, J. M.; Patterson, D. *Polymer* **1969**, *10*, 247.
- (11) Flory, P. J.; Eichinger, B. E.; Orwoll, R. A. *Macromolecules* **1968**, *1*, 287.
- (12) (a) Martuscelli, E.; Silvestre, C.; Bianchi, L. *Polymer* **1983**, *24*, 1458. (b) Bianchi, L.; Cimmino, S.; Forte, A.; Greco, R.; Martuscelli, E.; Riva, F.; Silvestre, C. *J. Mater. Sci.* **1985**, *20*, 895.
- (13) Hammouda, B.; Krueger, S.; Glinka, C. *J. Res. Natl. Inst. Stand. Technol.* **1993**, *98*, 31.
- (14) Walsh, D. J.; Graessley, W. W.; Datta, S.; Lohse, D. J.; Fetters, L. J. *Macromolecules* **1992**, *25*, 5236.
- (15) Hayashi, H.; Flory, P. J.; Wignall, G. D. *Macromolecules* **1983**, *16*, 1328. See also Flory, P. J. *Statistical Mechanics of Chain Molecules*; Hanser: New York, 1988, for the temperature coefficient of chain dimensions in polyisobutylene.
- (16) Crist, B., private communication.
- (17) Hildebrand, J. H.; Scott, R. L. *The Solubility of Non-Electrolytes*, 3rd ed.; Dover Publications: New York, 1964.
- (18) Allen, G.; Gee, G.; Wilson, G. J. *Polymer* **1960**, *1*, 456. Allen, G.; Gee, G.; Margaraj, D.; Sims, D.; Wilson, G. J. *Polymer* **1960**, *1*, 467.
- (19) Eichinger, B. E.; Flory, P. J. *Macromolecules* **1968**, *1*, 285.
- (20) Krishnamoorti, R.; Graessley, W. W.; Dee, G. T.; Walsh, D. J.; Fetters, L. J.; Lohse, D. J., manuscript in preparation.
- (21) Patterson, D.; Robard, A. *Macromolecules* **1978**, *11*, 690.
- (22) Jancso, G.; Rebelo, L. P. N.; Van Hook, W. A. *Chem. Rev.* **1993**, *93*, 2645.

MA941265Z